13th IEA Heat Pump Conference
April 26-29, 2021 Jeju, Korea

Optimization of Phase Change Thermal Energy Storage Unit Based on a New Thermal Resistance Model

Lingkun Liu[a], Xiangfei Liang[a,b,*]

[a]Refrigeration Institute of Gree Electric Appliances, Inc.of Zhuhai, Zhuhai 519070, China
[b]National Engineering Research Center of Green Refrigeration Equipment, Zhuhai 519070, China

Abstract

Considering the lack of the heat transfer behavior calculation methods of the phase change thermal energy storage (PCTES) unit, a new comprehensive model based on the effective thermal resistance coupled with heat transfer temperature difference is established and validated by CFD results. The effects of relative physical properties of the phase change material (PCM) and all the configuration parameters of the PCTES unit have been implemented into the model. It is proved that the average heat transfer rate and time duration for the PCM to be fully melt/solidified can be well predicted. To achieve better heat transfer behavior and larger heat storage density with acceptable cost, the optimization of fin-and-tube PCTES unit is established. Based on the average heat transfer rate per unit cost, the recommended structural parameters and PCM properties for PCTES unit are given.

Selection and/or peer-review under responsibility of the organizers of the 13th IEA Heat Pump Conference 2020.

Keywords: Phase change material; Thermal energy storage; Thermal resistance model; Parameters optimization

NOMENCLATURE

c_p	Specific heat ($Jkg^{-1}K^{-1}$)	**Greek symbols**	
F_p	Fin pitch (m)	δ	Thickness (m)
h	Heat transfer coefficient ($Wm^{-2}K^{-1}$)	γ	Phase change fraction
L	Tube length (m)	λ	Thermal conductivity ($Wm^{-1}K^{-1}$)
M	Mass (kg)	μ	Dynamic viscosity (Pas)
P	Heat transfer rate (W)	ρ	Density (kgm^{-3})
P_t	Transversal tube pitch (m)		
P_l	Longitudinal tube pitch (m)	**Subscripts**	
Q	Heat (J)	ave	Average value
r	Radius (m)	fluid	Heat transfer fluid inside tube
r_e	Characteristic radius (m)	mush	Mushy zone
R	Thermal resistance (KW^{-1})	in	Tube inner wall
t	Time-consuming of phase change (s)	out	Tube outer wall
T	Temperature (K)	out2	Fin collar outer wall
y	Coordinate in gravity direction (m)	pci	Phase change interface
m,n,l	Empirical constant in the model	PCM	Phase change material

1. Introduction

As a new thermal energy storage medium, phase change material (PCM) has been widely used in energy peak-to-valley transfer, building energy conservation, industrial waste heat recovery, electronic device heat dissipation, etc [1]. Phase change materials are generally classified into low temperature phase change

* Corresponding author. Tel.: +86-756-8589554; fax: +86-756-8668982.
E-mail address: liangxf@cn.gree.com.

materials (less than 80℃), medium temperature phase change materials (80-200℃) and high temperature phase change materials (above 200℃). Medium and low temperature PCMs have been widely used in various thermal energy storage systems [2]. In applications, the thermal performance of thermal energy storage systems is limited by the low thermal conductivity, subcooling and phase separation of PCMs. Fan and Khodadadi [3] summarized the experimental and theoretical approaches of enhancing the thermal conductivity of PCM in past studies. Safari et al. [4] summarized the effects of subcooling on the thermal performance of phase-change energy storage systems, analyzed various methods to improve or control the degree of subcooling, and conducted a method for optimizing the phase-change energy storage system with subcooling. Gunasekara et al. [5] analyzed the phase change properties of PCMs from the perspective of phase diagram based on phase equilibrium theory, and summarized the causes of instability of phase change systems and methods to solve them. In addition to directly improving the performance of the PCM, the optimization of the thermal energy storage device, such as the addition of fins and the improvement of its structure, has also become a research aspect [6]. Chang et al. [7] studied the variation of the heat transfer coefficient outside the small-diameter light tube with different structural arrangements.

For the theoretical and numerical study of the phase change process of PCMs, Neumann [8] obtained the analytical solution of the semi-infinite large plane case by the mathematical method. Subsequent studies have been applied to more complex situations. With the development of numerical methods, various physical models have emerged to replace mathematical analytical solutions, which can be applied to any complex geometric conditions. Voller [9] proposed a melting/solidification model based on a fixed grid method. The energy equation is expressed by enthalpy, and a mushy zone constant is used to solve the momentum transfer near the phase change interface. Further, Chen et al. [10] studied the effect of this mushy zone constant on melting/solidification characteristics and overall heat transfer performance. Meanwhile, various simplified phase-change thermal models have also been applied by various building energy analysis software [11].

When studying a specific type of TES device filled with PCM, the thermal resistance model based on the heat flow is also proposed and improved due to its simplicity and good reliability. Tay et al. [12] proposed a thermal resistance model of a flat fin-and-tube PCTES unit, which splits the heat flow into an isothermal heat flow and a parallel heat flow, and correspondingly establishes the corresponding thermal resistance network. An empirical constant P factor is used to calculate the ratio of the two heat fluxes. The model can be used for thermal resistance analysis and evaluate the efficiency of the heat transfer unit using the Effectiveness-NTU method. Similarly for the flat fin-and-tube PCTES unit, Chen et al. [13] proposed a more concise parallel thermal resistance network model, which approximates the total transferred heat to the heat passing through the solid-liquid interface. This method does not require the P factor, and still possesses small deviations.

The effectiveness of the PCTES unit based on the above thermal resistance model is the integral average of thermal resistance with respect to coordinates. However, due to the complexity of the phase change interface migration, the method of calculating the thermal resistance is not very accurate, and whether its effectiveness can accurately reflect its thermal performance is still a problem [14]. Moreover, the model can not calculate the phase change time and heat transfer rate of the specific TES unit under specific working conditions. In this situation, for the common PCTES unit filled with PCM outside the tube, this work proposes a method for establishing the effective thermal resistance based on Chen's phase interface thermal resistance model, and cooperates with a PCM temperature distribution hypothesis.

2. Physical model

2.1. Basic thermal resistance model of fin-and-tube PCTES unit

The schematic diagram of the structure of the fin-and-tube heat exchanger arranged in a regular triangular cross row is shown in Fig.1(a). Considering the heat flow flowing through a heat storage unit, it can be divided into two paths as shown in Fig.1(b). A part of heat flows from the in-tube heat transfer fluid through the tube wall and the flanged fins into the PCM, and the rest flows through the tube wall and the protruding fins into the PCM [13]. The equivalent thermal resistance network is shown in Fig.2. The expressions of the thermal resistance of each part in a PCTES unit are as follows

$$R_{fluid}=\frac{1}{2\pi r_{in}Lh_{fluid}},\quad R_{tube}=\frac{ln(r_{out}/r_{in})}{2\pi L\lambda_{tube}},\quad R_{collar}=\frac{ln(r_{out2}/r_{out})}{2\pi L\lambda_{collar}},\quad R_{fin}=\frac{ln(r_e/r_{out})}{2\pi\delta_{fin}\lambda_{fin}} \tag{1}$$

$$R_{PCM,1} = \frac{(r_{pci} - r_{out2})/(r_e - r_{out2}) \cdot (F_p - \delta_{fin})/2}{\pi(r_e^{\,2} - r_{out2}^{\,2})\lambda_{PCM}} \tag{2}$$

$$R_{PCM,2} = \frac{ln(r_{pci}/r_{out2})}{2\pi(F_p - \delta_{fin})\lambda_{PCM}} \tag{3}$$

$$R_{PCM\&fin} = \left(\frac{1}{R_{fin} + R_{PCM,1}/2} + \frac{1}{R_{PCM,2}} \right)^{-1} \tag{4}$$

$$R_{total} = R_{fluid} + R_{tube} + R_{collar} + R_{PCM\&fin} \tag{5}$$

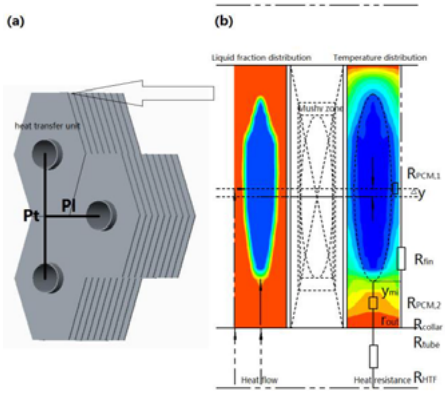

Figure 1 (a) Fin-and-tube heat exchanger structure (b) Fin-parallel cross section between two neighboring tubes of PCTES unit: heat flow paths (left), thermal resistance (right), liquid fraction distribution (left), solid-liquid interface approximation rectangular (middle) and temperature distribution (right)

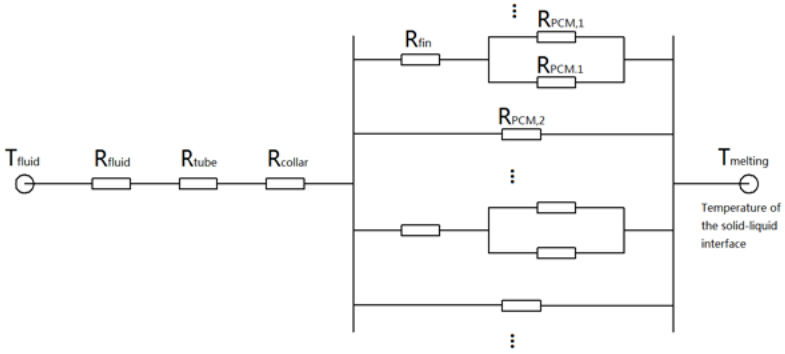

Figure 2 Schematic diagram of the thermal resistance network

In order to calculate the instantaneous heat transfer rate in the whole phase change process, it is also necessary to define the heat transfer temperature difference between the in-tube fluid and the PCM corresponding to the total thermal resistance of the network. The PCM temperature distribution assumption is brought out, where the PCM average temperature in the specific region is used as the PCM side characterization temperature, and the semi-theoretical semi-empirical corrections based on the CFD simulation results are carried out to obtain the outside-tube thermal resistance $R_{PCM\&fin.}$ For the sake of brevity, the following discussion is based on a single PCTES unit, ignoring the finless zone in the TES container.

2.2. Heat transfer temperature difference distribution assumption

The temperature distribution assumptions of the PCM depending on time and space are presented as follows.

(1) As shown in Fig.3(a), the phase change process is artificially divided into two periods noted as p1 and p2, the PCM enthalpy increment in the p1 period includes all sensible heat from the initial temperature to the melting point and partial latent heat. A rough approximation is used for the p1 period: when integrating time, the PCM average temperature and the phase change fraction are assumed to vary linearly with time, and the ratio of their variation rate is set to a constant value.

(2) Fig.1(b) shows the liquid fraction distribution (left side) and temperature distribution (right side) of the intermediate surface between the adjacent fins in the TES unit presented by the CFD simulation result. It is assumed that the temperature distribution law along the tube radial and fin normal direction of the PCM is the same.

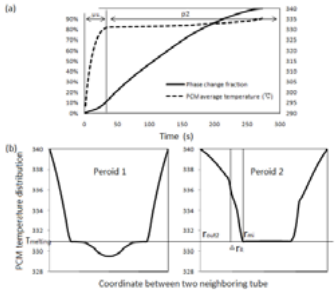

Figure 3 Schematic diagram of the (a) segmentation during a phase change process (b) PCM temperature distribution between neighboring heat transfer unit

(3) As shown in Fig.3(b), it indicates that during the p2 period, the temperature of the non-phase-change region has reached a constant value of $T_{melting}$. And in the already-phase-change region, it suggests that the equivalent PCM thermal resistance layer is thinned due to the temperature of the near-tube region has approached the fluid temperature. The thickness of the effective thermal resistance layer is approximated by an empirical formula:

$$\Delta r_R = m(r_{mi} - r_{out2}) \tag{6}$$

Where r_{mi} is the coordinate of the mushy zone inner interface, r_{out2} is the coordinate of outer wall of the fin flange and m is an empirical constant. In the region of r_{out2} to r_{mi}–Δr_R, the temperature is assumed to be equal to the fluid temperature T_f, and in the region *of* r_{mi}–Δr_R, the temperature distribution is

$$T(r) = (T_f - T_{melting})\frac{r - r_{mi}}{m(r_{out2} - r_{mi})} + T_{melting} \tag{7}$$

From the assumption (2), the average PCM temperature of the region corresponding to the effective thermal resistance is the expression of r_{mi}, denoted as $T_{eff}(r_{mi})$. Record the heat transfer temperature difference as $\Delta T_{eff}(r_{mi}) = T_f - T_{eff}(r_{mi})$, expressed by

$$\Delta T_{eff}(r_{mi}) = \frac{T_{melting} \cdot \pi(r_e^{\,2} - r_{mi}^{\,2}) + \int_{r_{mi}-\Delta r_R}^{r_{mi}} T(r) \cdot 2\pi r dr}{\pi[r_e^{\,2} - (r_{mi} - \Delta r_R)^2]} \tag{8}$$

2.3. Correction of thermal resistance outside the tube

The correction of the outer side thermal resistance from Eq.(4) includes these aspects: mushy zone correction; effective PCM thermal resistance layer correction; effective fin thermal resistance correction; TES unit shape correction; phase interface migration correction.

(1) Mushy zone correction

As shown in Fig.1(b), due to the amorphous nature of the specific PCM, resulting in a thin-layer solid-liquid interface instead of a sharp interface. In a common used solid-liquid phase enthalpy model [9], a mushy zone constant A_{mush} is used to reflect its amorphous nature. To describe this feature, a mushy zone shaped as a thin layer with the linearly distributed liquid fraction is established. The thickness of the mushy zone is described by the following correlation:

$$\Delta r_{mush} = n(r_{mi} - r_{out2}) \tag{9}$$

n is mainly affected by the mushy zone constant (which can be considered as a PCM inherent physical property) and viscosity. The data is fitted to the following relationship by CFD simulation results.

$$n = 0.5\left(A_{mush}^{\,1/3} \cdot \mu\right)^{-0.5} \tag{10}$$

Thus, the expression of the total phase change fraction of the PCM with respect to the interface coordinates r_{mi} in the mushy region can be obtained as $\gamma(r_{mi})$. Note that when the mushy zone advances to the boundary of the TES unit, the expression changes.

(2) Effective PCM thermal resistance layer correction

This correction has been described in Section 2.2. The two local thermal resistances corrected are

$$R_{eff,PCM,1}(r_{mi}) = \frac{\Delta r_R/(r_e - r_{out2}) \cdot (F_p - \delta_{fin})/2}{\pi(r_e^{\,2} - r_{out2}^{\,2})\lambda_{PCM}} \tag{11}$$

$$R_{eff,PCM,2}(r_{mi}) = \frac{ln[r_{mi}/(r_{mi} - \Delta r_R)]}{2\pi(F_p - \delta_{fin})\lambda_{PCM}} \tag{12}$$

(3) Effective fin thermal resistance correction

The fin thermal resistance calculated from Eq.(1) is the annular thermal resistance from the fin base to the fin tip, but the heat flow is through the side face of the fin. Thus the fin thermal resistance needs to be corrected. Assuming that the fin temperature distribution is linearly distributed in the radial direction, find the radial coordinate where the fin temperature is the mass average fin temperature. The annular thermal resistance from the fin base to the calculated coordinate is considered as the effective fin thermal resistance. Simplified expression is

$$R_{fin}=\frac{ln(r_e/r_{out2})}{2\pi\delta_{fin}\lambda_{fin}}\left(\frac{r_e^2}{r_e^2-r_{out2}^2}-\frac{1}{2ln(r_e/r_{out2})}\right) \quad (13)$$

(4) PCTES unit shape correction

As shown in Fig.4, the PCTES unit is divided into hexagons, since there is no analytical expression for the irregular hexagon shape factor, it is convenient to use the approximate ellipse to characterize the shape of PCTES unit. Its long and short axes are of a=2/3P$_l$ (horizontal direction) and b=1/2P$_t$ (gravity direction). It is assumed that the phase interface is from the outer wall of the tube at the beginning of the phase change, and gradually migrates to the end of the ellipse shown in Fig.4.

(5) Phase interface migration correction

As shown in Fig.4, due to the difference between solid and liquid density and natural convection, the low-density phase moves upward and the high-density phase moves downward, causing the overall migration Δy of the phase interface in the direction of gravity, mainly affected by the difference in solid-liquid density and PCM liquid viscosity. Fitting the CFD simulation results into a correlation:

$$\Delta y=(y_{mi}-y_{out2})[1-exp(-l\frac{\Delta\rho}{\mu})] \quad (14)$$

Where $\Delta\rho$ is the PCM density difference between solid and liquid phases in unit of kg/m^3, μ is the PCM liquid dynamic viscosity in unit of kg/m.s and l is an empirical constant.

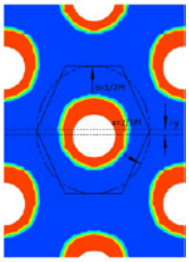

Fig.4 Schematic diagram of PCTES unit shape correction

So far, the total thermal resistance based on the effective PCM thermal resistance layer is obtained with respect to the boundary coordinate r of the mushy zone, and is denoted as $R_{eff,total}(r_{mi})$. The calculation of the instantaneous heat transfer rate can be done with the help of the previously obtained $\Delta T_{eff}(r_{mi})$ and $\gamma(r_{mi})$.

First, the total time of the phase change process is calculated by integration. The total enthalpy change of the PCM in each infinitesimal element period is equal to the total heat it receives:

$$t=\int_{t1|\gamma=\gamma1}^{t2|\gamma=\gamma2}dt=M_{PCM}\int_{\gamma=\gamma1}^{\gamma=\gamma2}\frac{C_p\cdot d\Delta T+LH\cdot d\gamma}{\Delta T_{eff}/R_{eff}}=M_{PCM}\int_{y_{mi2}|\gamma=\gamma1}^{y_{mi1}|\gamma=\gamma2}\frac{C_p\frac{\partial\Delta T}{\partial y_{mi}}+LH\frac{\partial\gamma}{\partial y_{mi}}}{\Delta T_{eff}/R_{eff}}dy_{mi} \quad (15)$$

Where y_{mi1} and y_{mi2} are interface coordinates in the y-direction mushy region corresponding to the phase change fractions γ1 and γ2 based on the expression of $\gamma(r_{mi})$. Similarly, the PCM average temperatures T1 and T2 corresponding to the phase change fractions γ1 and γ2 can be calculated from $T(r_{mi})$. Then the total transferred heat and average heat transfer rate of the considered process are

$$Q_{total}=M_{PCM}[C_p(T2-T1)+LH(\gamma2-\gamma1)] \quad (16)$$

$$P_{ave} = Q_{total} / t \tag{17}$$

Similarly, the time average of the effective heat transfer temperature difference and the effective thermal resistance can be integrated.

$$R_{eff,ave} = \int_{t1|\gamma=\gamma1}^{t2|\gamma=\gamma2} R_{eff}(y_{mi})dt \Big/ t \tag{18}$$

$$\Delta T_{eff,ave} = \int_{t1|\gamma=\gamma1}^{t2|\gamma=\gamma2} \Delta T_{eff}(y_{mi})dt \Big/ t \tag{19}$$

2.4. Model Validation

The CFD simulation on the fin-and-tube PCTES unit is as shown in Fig.6, the calculation domain includes the solid fin region and the solid-liquid PCM phase change region. The two regions are thermally coupled to each other, the upper and lower boundaries are periodic, and the left and right boundaries are symmetrical. Melting/solidification model is adopted and UDFs are used to set the changeable physical parameters. A series of non-steady-state phase change processes are simulated to fit the required empirical coefficients and relationships in this paper. After that, simulation results under arbitrary parameters and working conditions are used for the validation. The deviation between the CFD simulation and the model is shown in Table 1.

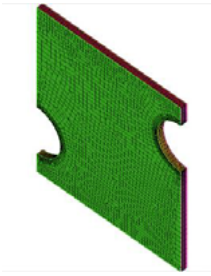

Fig.5 Mesh grid diagram of PCTES unit for CFD simulation

Table 1. Deviation between calculation model and CFD simulation results

		φ7 tube		φ6 tube	
		$\Delta T_{heating}$= 9K	$\Delta T_{heating}$= 6K	SAT	Paraffin
Phase change completed time-consuming (s)	CFD results	191	273	100	52.7
	Model results	198.42	279.53	100.21	51.20
	Deviation	3.88%	2.39%	0.21%	-2.85%
Average heat transfer rate (W/m^3)	CFD results	2.474E+06	1.700E+06	4.619E+06	3.662E+06
	Model results	2.468E+06	1.724E+06	4.781E+06	3.752E+06
	Deviation	-0.24%	1.41%	3.51%	2.46%

It can be seen that the model can accurately predict the heat transfer performance for different heat transfer conditions with variable structure parameters and PCM types. The deviation of the average heat transfer rate between the model results and CFD results is below 4%. It can be considered that the performance of the fin-and-tube PCTES calculated by this model is with enough accuracy and versatility.

3. PCTES unit structure parameters optimization

The thermal performances of the PCTES unit for the fin-and-tube under a constant wall temperature boundary condition are investigated. The focused performances are as follows: the PCTES unit cost C (RMB/m^3), the latent heat storage density (MJ/m^3) of the TES unit, and the average heat transfer rate P_{ave} (W/m^3) during the whole phase change process.

The latent heat storage density = PCM density × PCM volume fraction in the PCTES unit × PCM melting enthalpy

The PCTES unit cost = Tube cost + Fin cost + PCM cost

The average heat transfer rate = Total amount of transferred heat / Time-consuming during the whole phase change process

The latter two are combined to form a new performance that reflects the unit cost performance of the TES unit: heat transfer rate per unit cost = P_{ave}/C (W/RMB).

Table 2 shows the fixed parameters, the reference structure parameters and heat transfer conditions for the discussed fin-and-tube PCTES unit.

Table 2. Parameters set for the fin-and-tube PCTES unit calculation

Copper tube specifications	φ7(54g/m)	φ5(34.2g/m)	φ4(24.6g/m)
Reference structure parameters (mm)	Pt=22, Pl=19.05	Pt=19.05, Pl=16.5	Pt=14.7, Pl=13.8
	Fp=1.7, δ_{fin}=0.105	Fp=1.4, δ_{fin}=0.105	Fp=1.3, δ_{fin}=0.105
Working conditions	PCM initial temperature 15℃, $\Delta T_{heating}$= 9℃		
Material price (RMB/kg)	Copper (tube material): 50; Aluminum (fin material): 16;		
	PCM: Sodium acetate trihydrate (SAT): 5; Paraffin: 4；		

For the fin-and-tube, the change of structural parameters has much greater influence on the heat transfer rate than the energy storage density. Therefore, the influence on heat storage density is ignored. The heat transfer rate per unit cost under various structural parameters of different tube diameters is shown in Fig.6-8. The x, y, and z axes respectively represent the change of the transversal tube pitch, the longitudinal tube pitch, and the fin pitch of the PCTES unit structure, the pentagonal point is a commonly used structure. Each colored surface represents structural parameter combinations that possess the equal heat transfer rate per unit cost. The right side box compares the heat transfer rate per unit cost when the two PCMs are used under the reference structure at pentagonal point.

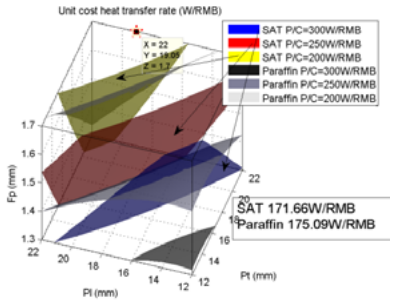

Figure 6 φ7 fin-and-tube PCTES unit cost performance with structural parameters

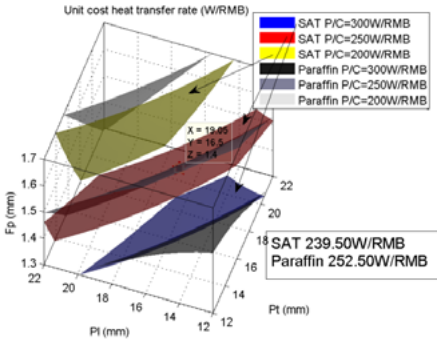

Figure 7 φ5 fin-and-tube PCTES unit cost performance with structural parameters

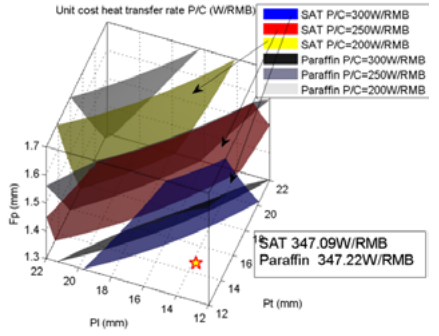

Figure 8 φ4 fin-and-tube PCTES unit cost performance with structural parameters

It can be seen that, the smaller the tube pitch and the fin pitch, the higher the heat transfer rate per unit cost. The influence of the transversal and longitudinal tube pitch is similar, and simultaneously reducing the transversal and longitudinal tube pitch is better than reducing only one of them. In the case of a large tube pitch, the fin pitch variation within the range of the figure has little effect on the heat transfer rate per unit cost, which is due to the effective fin thermal resistance expression of the annular fin thermal resistance in the equation (13). As the heat transfer unit characteristic radius re increases, it increases sharply and will dominate the thermal resistance outside the tube.

It can be seen that for paraffin and SAT used as PCM, the heat transfer rate per unit cost is very close to each other under the PCTES structure at pentagonal point. The decline in performance due to the low thermal conductivity and high viscosity of paraffin is compensated by its low mushy zone constant and low cost. But it should be noted that in terms of heat storage density, SAT is about (264*1300)/(168*830)=2.46 times of paraffin. Generally, the higher the thermal conductivity of PCM, the lower the viscosity, the stronger the amorphous and the larger the ratio of latent-sensible heat, the better the average heat transfer rate of the PCTES unit.

It can also be seen from the figure that the dependency of heat transfer rate per unit cost on the fin pitch is more obvious for paraffin than SAT. When the fin pitch is greater than 1.5 mm, the P/C=300 surface shrinks sharply inward, that is, with the increase in film distance, the heat transfer rate per unit cost drops dramatically. It can be explained that when the PCM thermal conductivity is low, and the $R_{PCM,1}$ and $R_{PCM,2}$ in the outside-tube thermal resistance of Eq.(4) occupy a larger proportion. After the fin pitch increases to a certain extent, the outside-tube thermal resistance increases sharply, causing the overall performance deteriorates drastically.

When the PCM is SAT, the heat transfer rate per unit cost of the φ7, φ5 and φ4 fin-and-tube PCTES units is 172W/RMB, 239W/RMB and 330W/RMB, respectively. It indicates that the unit cost performance will increase with the decrease of the tube diameter. And there is a similar increase when the PCM is paraffin.

Therefore, in the currently used size range of fin-and-tube heat exchangers, when used as a PCTES container, smaller diameter should be selected.

4. Conclusion

A physical model based on the thermal resistance network that can be used for the non-steady state heat transfer calculation of the PCTES unit is established. The model can predict average heat transfer rate under different structural parameters, heat transfer conditions and PCM types with high accuracy. The following conclusions can be summarized:

(1) The model extends the conventional thermal resistance analysis methods of PCTES unit, making the model available for the calculation of actual heat transfer rate. Further, it has small deviation from CFD simulation results and high computational efficiency, and can be used for multi-dimensional multi-objective optimization of PCTES unit.

(2) In the structural parameters range of fin-and-tube PCTES unit currently used, the smaller the tube pitch and the fin pitch, the higher the heat transfer rate per unit cost. The heat transfer rate per unit cost of φ4, φ5 and φ7 fin-and-tube PCTES unit is 172W/RMB, 239W/RMB and 330W/RMB, respectively. Therefore, for the 4-10 mm tube diameter range of fin-and-tube heat exchangers, when used as a PCTES container, structure parameters with smaller diameter should be selected.

(3) In the case of a large tube pitch, the fin pitch variation within the range of 1.3-1.7mm has little effect on the heat transfer rate per unit cost. And its dependency on the fin pitch is more sensitive for the PCM with low thermal conductivity than that with high thermal conductivity. For paraffin and SAT used as PCM, the heat transfer rate per unit cost is coincidentally very close to each other under several commonly used PCTES structure.

References

[1] Tao YB, He YL. A review of phase change material and performance enhancement method for latent heat storage system. Renewable and Sustainable Energy Reviews 2018;93:245–259.
[2] Sharma A, Tyagi VV, Chen CR, Buddhi D. Review on thermal energy storage with hase change materials and applications. Renewable and Sustainable Energy Reviews 2009;13:318–45.
[3] Fan L, Khodadadi JM. Thermal conductivity enhancement of phase change materials for thermal energy storage: a review. Renewable and Sustainable Energy Reviews 2011;15:24–46.
[4] Safari A, Saidur R, Sulaiman FA, Xua Y, Dong J. A review on subcooling of Phase Change Materials in thermal energy storage systems. Renewable and Sustainable Energy Reviews 2017;70:905–919.
[5] Saman Nimali Gunasekara, Viktoria Martin, Justin Ningwei Chiu. Phase equilibrium in the design of phase change materials for thermal energy storage: State-of-the-art. Renewable and Sustainable Energy Reviews 2017;73:558–581.
[6] Merlin K, Delaunay D, Soto J, Traonvouez L. Heat transfer enhancement in latent heat thermal storage systems: Comparative study of different solutions and thermal contact investigation between the exchanger and the PCM. Applied Energy 2016;166:107–116.
[7] Chang NC, Li CJ, Wang CC. Performance of bare-tube bundle having small diameter tube: with and without partial bypass. International Communications in Heat and Mass Transfer 2015;67:73–80.
[8] Weker P, Mineur JM. A performance index for thermostatic radiator valves. Applied Energy 1980;6:203–215.
[9] Voller VR. A fixed grid numerical modeling methodology for convection-diffusion mushy region phase-change problems. International Journal of heat Mass Transfer 1987;30(8):1709–1719.
[10] Chen YL, Peng CH, Guo Y. Experimental and numerical study on melting process of paraffin in a vertical annular cylinder. Thermal Science 2019;23(2A):525–535.
[11] Sole CA. An overview on design methodologies for liquid-solid PCM storage systems. Renewable and Sustainable Energy Reviews 2015;52:289–307.
[12] Tay NHS, Belusko M, Castell A, Cabeza LF, Bruno F. An effectiveness-NTU technique for characterising a fin-and-tubes PCM. Applied Energy 2014;131:377–385.
[13] Chen H, Liang XF, Wu YW. Thermal resistance analysis for fin-and-tube phase change thermal energy storage unit. Proceedings of the 25th IIR International Congress of Refrigeration; ID:1440.
[14] Groulx D. The rate problem in solid-liquid phase change heat transfer: efforts and questions toward heat exchanger design rules. Proceedings of the 16th International Heat Transfer Conference 2018;IHTC–16:KN23.